IEEE Access
Multidisciplinary | Rapid Review | Open Access Journal

Received July 23, 2020, accepted August 22, 2020, date of publication September 3, 2020, date of current version September 17, 2020.

Digital Object Identifier 10.1109/ACCESS.2020.3021503

Twisted Beams With Variable OAM Order and Consistent Beam Angle via Single Uniform Circular Arrays

PAOLO BURGHIGNOLI[1], (Senior Member, IEEE), WALTER FUSCALDO[1], (Member, IEEE), FRANCESCO MANCINI[2], DAVIDE COMITE[1], (Senior Member, IEEE), PAOLO BACCARELLI[3], (Member, IEEE), AND ALESSANDRO GALLI[1], (Member, IEEE)

[1]DIET Department, Sapienza University of Rome, 00148 Rome, Italy
[2]Leonardo S.p.A., Electronics, 12400 Rome, Italy
[3]Department of Engineering, University of Rome Tre, 00146 Rome, Italy

Corresponding author: Paolo Burghignoli (paolo.burghignoli@uniroma1.it)

ABSTRACT A planar antenna radiating twisted beams with different azimuthal order and a consistent beam angle is designed by employing a single uniform circular array embedded in a Fabry–Perot cavity. Circular phased arrays placed in free space are commonly employed to radiate conical beams carrying orbital angular momentum. However, the beam angle depends on both the array radius and the azimuthal order of the beam, thus requiring the use of multiple concentric circular arrays in order to produce beams with different azimuthal order and a common beam angle. In the proposed design, this is simply achieved by exciting higher-order cylindrical leaky waves through a single circular array feeding a Fabry-Perot cavity. Such waves radiate conical patterns whose beam angle is mainly determined by the relevant radial wavenumber and only weakly depends on the azimuthal order. In particular, we propose here an antenna design capable of radiating beams with azimuthal orders 0, ± 1, ± 2, and ± 3 in the microwave range. The cavity is fed by an array of coaxial probes optimized for input matching through the inclusion of parasitic metal pins. Numerical full-wave simulations validate the effectiveness of the proposed design in terms of radiation patterns, passive input scattering parameters, and active input reflection coefficients.

INDEX TERMS Circular arrays, cylindrical waves, leaky waves, Fabry–Perot cavities, orbital angular momentum, planar antennas, partially reflecting surfaces.

I. INTRODUCTION

Twisted electromagnetic waves have been the subject of intense investigations in the last decades since the seminal paper by Allen *et al.*, where optical beams with helical wavefronts were shown to carry orbital angular momentum (OAM) [1]. Applications of such OAM waves have been investigated in all frequency ranges, from radio frequencies to optics, X- and gamma-rays [2]. They range from physics (e.g., micromanipulation with optical tweezers [3], [4]) and quantum computing (e.g., quantum information processing [5]–[7]) to, more recently, wireless and wired communication systems (although with some controversies; see, e.g., [8], [9] and references therein) as well as radar and imaging systems [10]–[12].

The associate editor coordinating the review of this manuscript and approving it for publication was Mohammad Zia Ur Rahman.

As concerns radio frequencies, different types of antennas for generating OAM beams have been proposed, operating from the microwave to the millimeter-wave ranges. These systems include spiral phase plates and their variants [13]–[16], twisted parabolic reflectors [17]–[19], circular traveling-wave antennas [20], [21], slot antennas [22], reflectarrays [23], metasurfaces [24]–[27], photonic crystals [28], helical antennas [29], planar arrays via radiation matrix eigenfields [30].

However, by far the most versatile method for producing OAM beams is based on Circular Arrays (CAs) [31]–[40]. In fact, by properly phasing the array elements, it is possible to readily reconfigure the array operation and hence switch from one OAM order to another, as well as to simultaneously operate on multiple OAM orders.

CAs have found recent applications in vortex imaging systems [11], [12], [37], [41]–[44], where the simultaneous use

of multiple OAM orders allows for increasing the azimuthal resolution. In this frame, it is important to ensure that the elevation pattern be *consistent* among all the excited OAM orders. However, CAs operating in free space produce twisted conical patterns whose beam angle is strongly dependent both on the array radius and on the OAM order. Hence, the use of multiple, concentric CAs (Concentric Uniform CAs, CUCAs) has been proposed [41], [42], [44], where each CA radiates a different OAM order with the same beam angle.

In this paper we aim at showing that the same result, i.e., consistent beam angle among different OAM orders, can be achieved by using a *single uniform* CA (SUCA), provided that the array is not placed in free space (cf. Fig.1(a)) but inside a Fabry–Perot cavity (cf. Fig.1(b)). In fact, such a cavity supports *leaky modes*, that may be excited by the SUCA in the form of cylindrical leaky waves (CLWs) propagating radially with a complex wavenumber $k_\rho = \beta - j\alpha$. If the reflectivity of the PRS is high, a weakly attenuated CLW can be excited, which dominates the aperture field of the antenna; such CLW produces a main beam in the radiation pattern whose angular position is essentially determined by the leaky-mode phase constant β [45]–[49], and is thus almost independent of the OAM azimuthal order ℓ, at least for small values of ℓ.

The paper is organized as follows. In Sec. II the operating principle of the antenna is illustrated. In Sec. III the antenna design is reported. Numerical full-wave simulations are given in Sec IV in order to validate the effectiveness of the proposed design, in terms of radiation patterns as well as passive and active input antenna parameters. Conclusions are drawn in Sec. V.

II. OPERATING PRINCIPLE

The proposed antenna employs a uniform circular phased array embedded within a Fabry–Perot cavity antenna (FPCA) structure formed by a dielectric layer of thickness h and relative permittivity ε_r, bounded at the bottom by a metal ground plane and on top by a partially reflecting surface (PRS), as shown in Fig.1(b).

We will assume that the PRS is formed by a metal patterned screen of negligible thickness, e.g., a metal patch array or a slot array etched in a thin metal plate. The periodicity of the screen along the x and y axes is assumed to be much smaller than any relevant wavelength, so that the PRS can be represented as a *homogenized isotropic sheet*, characterized in the spectral domain by a surface (transition) admittance dyadic $\underline{\mathbf{Y}}_{\mathrm{PRS}}$. Here, we will limit our analysis to those PRSs whose dyadic admittance can be reduced to a single scalar value Y_{PRS} by virtue of negligible TE-TM coupling and almost polarization-independent behavior, such as those analyzed, e.g., in [50], [51].

The feeding array is assumed to be simply constituted by N coaxial probes penetrating the cavity from the bottom ground plane at $z = 0$, arranged along a circle of radius a centered on the z-axis, at the azimuthal angles $\phi_i = i2\pi/N$, $i = 0, 1, \ldots, (N-1)$. The complex excitation coefficients of

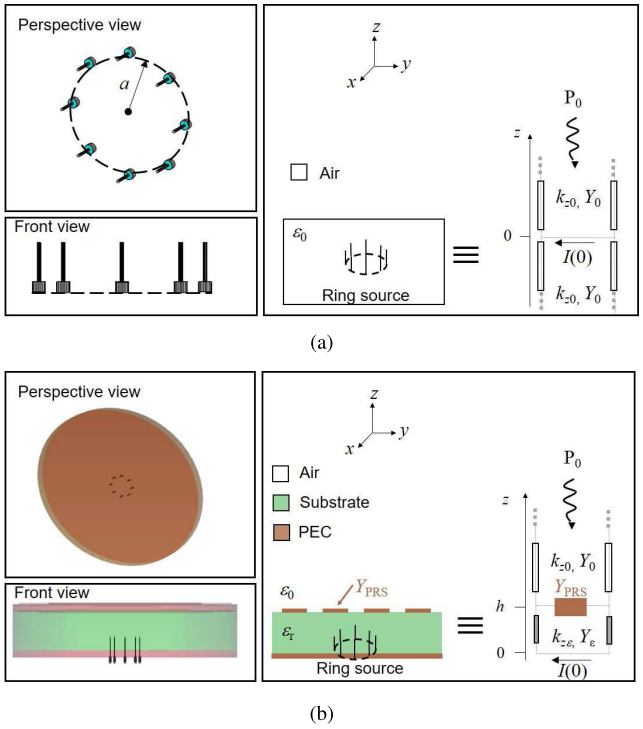

FIGURE 1. Perspective view, 1-D section, and transmission-line model of (a) a ring source radiating in free-space, and (b) a Fabry–Perot cavity antenna fed by a ring source.

the uniform array should then be $I_i = \exp(-j\ell\phi_i)$ in order to radiate the ℓ-th OAM order.

As far as the radiation pattern of the antenna is concerned, the probes can safely be modeled as vertical electric dipoles (VEDs). Furthermore, in order to simply illustrate the radiation mechanism, the discrete arrangement of VEDs will be replaced by a continuous distribution (a ring) of vertical impressed currents:

$$\mathbf{J}_{\mathrm{ring}} = P_0 \mathbf{z}_0 \frac{\delta(\rho - a)}{a} e^{-j\ell\phi} \delta(z) \tag{1}$$

where $\delta(\cdot)$ is the Dirac delta distribution, (ρ, ϕ, z) are the standard cylindrical coordinates, $\mathbf{z}_0$ is the unit vector of the z-axis, and P_0 (A·m) is a complex amplitude coefficient. Note that the use of a continuous source in place of the actual, discrete one neglects the excitation of higher-order azimuthal harmonics; these can however be minimized in practice by a proper design of the array radius a and number of elements N (the interested reader can find details in [49]).

The considered source, being constituted by vertical electric currents, excites a purely TM^z field whose cylindrical components depend on ϕ as $\exp(-j\ell\phi)$, by the rotational symmetry of the configuration. The electric field in the far region is therefore vertically polarized and has a conical pattern that can be written in the form

$$E_\theta(r, \theta, \phi) = E_0(r) P(\theta) e^{-j\ell\phi} \tag{2}$$

where $E_0(r) = jk_0\eta_0 \exp(-jk_0 r)/(4\pi r)$ (k_0 and η_0 being the free-space wavenumber and characteristic impedance,

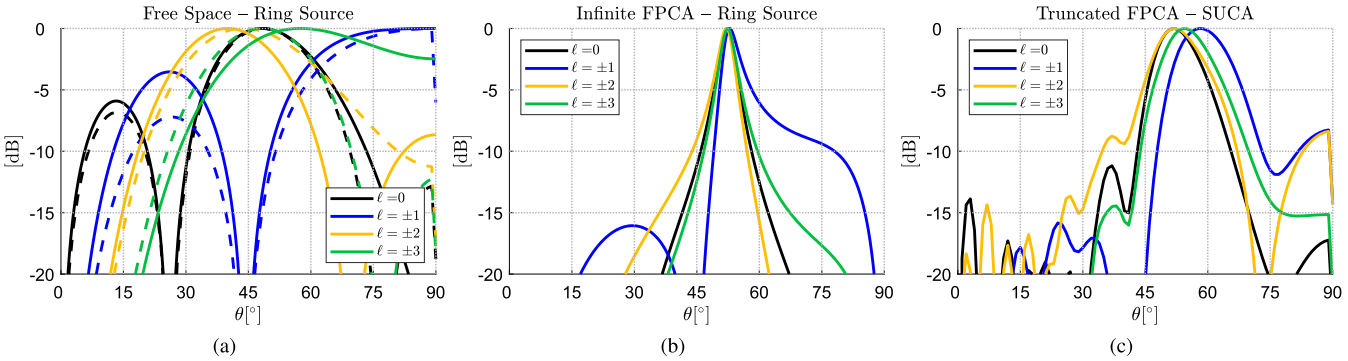

FIGURE 2. (a) and (b): Normalized far-field patterns in an arbitrary elevation plane for different OAM orders ℓ for a ring of vertical electric currents as in (1) placed (a) in free space, and (b) embedded in a single-layer, homogeneous FPCA supporting a TM leaky mode that radiates a conical beam pointing at about 52° at $f = 18$ GHz. *Parameters*: $h = 12.14$ mm, $\varepsilon_r = 1.2$, $a = 14.5$ mm. (c) Normalized far-field patterns for a multilayer FPCA supporting a TM leaky mode that radiates a conical beam pointing at about 55°, excited by a SUCA with $N = 8$ elements and truncated at $\rho = \rho_{max} = 109.5$ mm, in the plane $\phi = 0°$.

respectively), $P(\theta)$ is a pattern function in the elevation plane, and (r, θ, ϕ) are standard spherical coordinates.

The operating principle of the proposed antenna can be explained in terms of the effect on $P(\theta)$ of the environment where the vertical current ring (1) is placed. In fact, if the ring were placed in free space one would find (see Appendix A for details)

$$P^{\mathrm{FS}}(\theta) = -2\pi j^{\ell} P_0 \sin\theta J_{\ell}\left(k_0 a \sin\theta\right) \tag{3}$$

i.e., as is well known, the pattern would be described by a Bessel function of order ℓ and argument $k_0 a \sin\theta$. Now, by varying ℓ, the maxima of such functions are attained at different values of their argument and hence at different elevation angles θ. Hence, beams with different OAM order would have different beam angles, as it can be observed in Fig. 2(a).

Instead, if the ring source (1) is placed inside the FPCA, the pattern function becomes (see Appendix A for details)

$$P^{\mathrm{FP}}(\theta) = \frac{2\cos\theta \csc\left(k_{z\varepsilon} h\right) P^{\mathrm{FS}}(\theta) e^{jk_0 h\cos\theta}}{j\hat{k}_{z\varepsilon}\left(1 + \cos\theta \bar{Y}_{\mathrm{PRS}}\right) + \varepsilon_r \cos\theta \cot\left(k_{z\varepsilon} h\right)} \tag{4}$$

where $\hat{k}_{z\varepsilon} = k_{z\varepsilon}/k_0 = \sqrt{\varepsilon_r - \sin^2\theta}$, and $\bar{Y}_{PRS} = Y_{PRS}\eta_0$ represents the normalized admittance of the PRS (the bar and the hat refer to the normalization to η_0 and k_0, respectively). From (4) we note that now the pattern function goes to zero at the horizon, i.e., in the endfire direction $\theta = \pi/2$, in agreement with the Karp-Karal lemma [52]. But, more importantly, the resonant denominator in (4) is now capable of completely *reshaping* the pattern in the elevation plane.

This is exactly what occurs when a weakly attenuated TM fast leaky mode is supported by the FPCA, since then the relevant complex zero at $k_{\mathrm{LW}} = \beta - j\alpha$ of the denominator, considered as a function of $k_\rho = k_0 \sin\theta$, would be located close to the visible region between 0 and k_0 of the real k_ρ-axis and it would thus produce a resonant spike in the elevation pattern. Then, provided that the azimuthal order ℓ is not exceedingly large and hence the progressively flattening portion near the origin of the Bessel function $J_{\ell}\left(k_\rho \rho\right)$ in $P^{\mathrm{FS}}(\theta)$ washes out the leaky resonant spike, the net effect is that of a beam maximum located at the leaky beam angle $\theta_p \simeq \sin^{-1}\left(\beta/k_0\right)$, *independent of the OAM order* ℓ, as it can be observed in Fig. 2(b). (A detailed analysis of these aspects can be found in [48].)

III. ANTENNA DESIGN

A. FABRY-PEROT CAVITY DESIGN

In order to quantitatively assess the effectiveness of the innovative idea described above, the starting point for the design of the Fabry-Perot cavity has been a structure constituted by a grounded dielectric slab relative permittivity 1.2, covered by a thin periodic metal PRS, and operating at $f = 18$ GHz.

The indicated value of the relative permittivity is sufficiently larger than one so as to make the undesired quasi-TEM mode supported by the cavity a slow wave and hence reduce its spurious radiative effects on the antenna pattern at the operating frequency [49], [53]. However, since that value does not correspond to any commercial material, a multilayer design for the cavity has been adopted, in order to synthesize an effective permittivity approximately equal to the desired one by employing commercially available laminates [54]. In particular, a three-layer configuration has been selected, constituted by two sheets of RT Duroid 5880 with relative permittivity 2.2 and thickness 1.57 mm, separated by a thick foam layer with relative permittivity 1.04 and thickness 9 mm; the resulting multilayered cavity has thus a total thickness of 12.14 mm. Note that the relevant dispersion curves of the preliminary single-layer design and the multilayer design are rather similar around the operating frequency, as can be inferred from Fig. 3 [54].

As concerns the PRS, a 2-D periodic arrangement of square metal patches has been used, with spatial period $p = 3$ mm along both the x and y axes and spacing $s = 50\,\mu m$ between adjacent patches. Since $p = 0.18\lambda_0$ at $f = 18$ GHz, the PRS can be homogenized and represented by a TM surface admittance Y_{PRS}; by neglecting the metal losses, this will be a capacitive susceptance $Y_{\mathrm{PRS}} = j\omega C_{\mathrm{PRS}}$. The equivalent

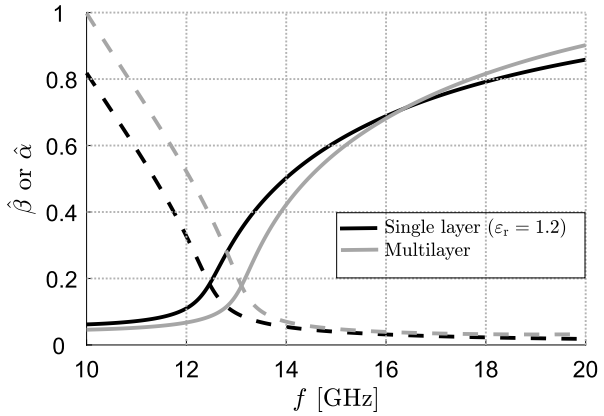

FIGURE 3. Normalized phase constants ($\hat{\beta} = \beta/k_0$) and attenuation constants ($\hat{\alpha} = \alpha/k_0$) of the fundamental TM leaky mode for both the single-layer, homogeneous FPCA and the multilayer FPCA.

capacitance of the PRS can accurately be estimated through the analytical formula [51]

$$C_{\rm PRS} = \frac{2p}{\pi \eta_0 \, c} \frac{\varepsilon_r^{\rm eff} + 1}{2} \ln \csc \left(\frac{\pi s}{2p} \right) \tag{5}$$

where $\varepsilon_r^{\rm eff} = 1.6$ is an effective relative permittivity, equal to the arithmetic average of the vacuum permittivity (1) and of the permittivity of the Duroid layer supporting the PRS (2.2), and c is the light velocity in vacuum. With the considered physical parameters, it results $C_{\rm PRS} \simeq 98.6$ fF, corresponding to a normalized PRS admittance $\bar{Y}_{\rm PRS} = j4.20$ at the operating frequency $f = 18$ GHz.

Once the equivalent admittance of the PRS is available, a standard transverse-resonance analysis of the entire structure can be carried out in order to derive the dispersion equation of the TM modes supported by the cavity [55]. This is then solved numerically in the complex plane, in order to determine the (generally complex) modal wavenumbers $k_\rho = \beta - j\alpha$. In particular, the designed antenna operates on the $\rm TM_1$ mode, for which $\beta/k_0 \simeq 0.816$ and $\alpha/k_0 \simeq 0.032$ at $f = 18$ GHz. The corresponding beam angle is $\theta_p \simeq \sin^{-1}(\beta/k_0) \simeq 55°$; this is just slightly larger than the beam angle for a homogeneous FPCA with $\varepsilon_r = 1.2$, for which $\beta/k_0 \simeq 0.792$ and $\alpha/k_0 \simeq 0.023$ at $f = 18$ GHz, so that the beam angle is $\theta_p \simeq \sin^{-1}(\beta/k_0) \simeq 52°$, as it can be inferred from Fig. 2(b).

B. FEEDER DESIGN

The antenna feeder is constituted by a phased array of N coaxial probes penetrating the cavity through the bottom ground plane at $z = 0$, equispaced along a circle of radius a and center at the origin. The antenna is designed to efficiently excite OAM orders with $|\ell| \leq \ell_{\rm max} = 3$.

According to the guidelines proposed in [49], the array radius has to be selected so that the excitation coefficient of the undesired quasi-TEM cavity mode is much smaller than the excitation coefficients of the desired $\rm TM_1$ mode, for all the azimuthal orders 0, ±1, ±2, and ±3. Furthermore, the wave impedances of the desired modes have to be predominantly resistive, in order to make the input matching of the feeding ports easier. Considering these criteria, a value $a = 14.5$ mm has been selected.

As concerns the number of elements N, the analysis in [49] shows that a lower bound is provided by the Nyquist criterion: $N \geq 2\ell_{\rm max} = 6$. However, larger values should be used to reduce the excitation of undesired higher azimuthal harmonics to negligible values; for the present design, the value $N = 8$ has been selected.

As concerns the coaxial probes, they have outer radius equal to 1 mm, inner radius equal to 0.3 mm, and length 4 mm above the ground plane. In order to minimize both the reflection coefficients at the ports and the level of mutual coupling among them, parasitic vertical vias of radius 0.37 mm and length 3.60 mm have been included, inserting them on a circle of radius 15.7 mm, slightly larger than but concentric with the array circle, in between each pair of adjacent elements.

IV. NUMERICAL RESULTS

In this section, full-wave results obtained with CST Microwave Studio are reported for both the radiation patterns of the FPCA and the relevant input parameters at the SUCA ports, in order to validate the effectiveness of the proposed design.

The simulated FPCA has a finite size, being laterally truncated at $\rho = \rho_{max} = 109.5$ mm; considering the value of the normalized attenuation constant of the operating leaky mode ($\alpha/k_0 = 0.032$ at $f = 18$ GHz), the resulting radiation efficiency of the antenna is 90 %. We should stress here that, in spite of its relatively large radiation efficiency, a truncated FPCA will radiate beams with appreciably larger beamwidths with respect to an ideally infinite FPCA, however with almost the same beam angle (see, e.g., [48, Fig. 7], [53, Fig. 3]).

A. RADIATION PATTERNS

In Fig. 2(c), normalized radiation patterns in the elevation plane $\phi = 0°$ are reported for the twisted beams radiated by the designed structure, obtained with CST Microwave Studio.

As a consequence of the lateral truncation, endfire radiation is no longer zero, mainly due to edge diffraction by the quasi-TEM mode supported by the FPCA, whose excitation coefficient is not exactly zero. Similar spurious radiative effects have been observed in [53], [54], where they have been experimentally suppressed by using lateral absorbers. Their complete elimination could be achieved by inserting inside the cavity layers of suitable materials, such as the wire medium, capable of suppressing the quasi-TEM mode [56]; this would, however, considerably complicate the overall design.

As a further consequence of the finiteness of the antenna aperture plane, the beamwidths of the patterns are larger than the corresponding ones for a laterally infinite structure (cf. Fig. 2(b)). The beam angles, however, remain stable by varying the azimuthal order, with a maximum squint of about $\pm3°$, greatly reduced with respect to the free-space

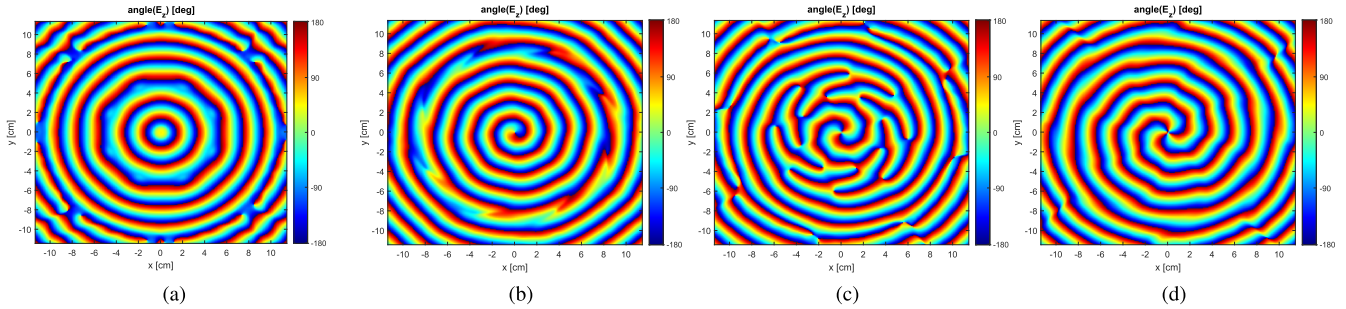

FIGURE 4. Phase distributions of the E_z component of the radiated electric field on the plane $z = 4.8$ mm for the OAM orders (from left to right) $\ell = 0, 1, 2, 3$.

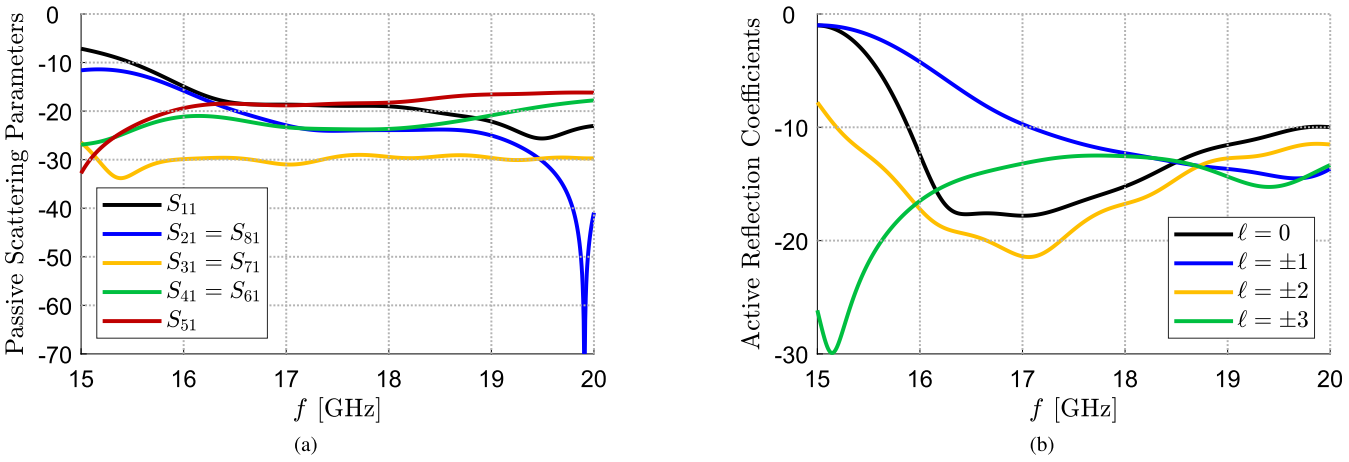

FIGURE 5. Input parameters of the SUCA, calculated with CST: (a) passive scattering parameters; (b) active reflection coefficients for the azimuthal orders $\ell = 0, \pm1, \pm2, \pm3$. ***Parameters***: as in Fig. 2.

case (cf. Fig. 2(a)). The maximum directivities of the patterns are also very stable with the azimuthal order, being equal to 10.28, 9.00, 9.24, 9.62 dB for $\ell = 0, \pm1, \pm2, \pm3$, respectively.

As concerns the azimuthal variation of the conical twisted beams, the maximum oscillation range of the patterns as a function of the azimuthal angle ϕ, evaluated at the maximum beam angle in elevation, are of 0.12, 0.7, 1.5, 1.7 dB for $\ell = 0, \pm1, \pm2, \pm3$, respectively. Such low values confirm that the number of array elements ($N = 8$) is sufficient to achieve a high degree of omnidirectionality for each OAM order.

Finally, near-field maps are reported in Fig. 4 for the phase of the E_z component of the radiated electric field, evaluated on the plane $z = 4.8$ mm, for $\ell = 0, 1, 2, 3$, to validate the generation of the desired OAM orders.

B. INPUT PARAMETERS

The passive scattering parameters S_{ij} $(i, j = 1, \ldots, 8)$ are reported in magnitude and in dB in Fig. 5(a). The symmetry of the configuration is such that the scattering matrix is circulant, so only S_{i1} $(i = 1, \ldots, 8)$ are reported; furthermore, $S_{21} = S_{81}$, $S_{31} = S_{71}$, $S_{41} = S_{61}$. At the operating frequency $f = 18$ GHz, both the input reflection coefficients S_{ii} $(i = 1, \ldots, 8)$ and the mutual transmission coefficients S_{ij} $(i \neq j)$ are below -18 dB in absolute value, thus showing an excellent level of input matching at the SUCA ports as well as a very low level of mutual coupling among different ports.

This is further confirmed by the values of the active input reflection coefficients, reported in Fig. 5(b): as it can be seen, at $f = 18$ GHz they are well below -10 dB for all the considered OAM orders.

V. CONCLUSION

A Fabry–Perot cavity antenna fed by a single uniform circular array of vertical coaxial probes has been designed for operation at microwave frequencies, capable of radiating conical patterns with different OAM orders (from 0 to ±3). Contrasted with alternative OAM antennas based on circular arrays operating in free space, whose beam angle strongly varies with the OAM order, the proposed OAM design offers a consistent beam angle. Numerical full-wave simulations have validated the design, which may find application in OAM-based radar or imaging systems, as well as in short-range OAM-based communication systems.

APPENDIX
DERIVATION OF THE PATTERN FUNCTIONS

In this Appendix the pattern functions (3) and (4) will be derived, produced by the continuous phased ring of vertical currents in (1) when placed in free space and inside an FPCA, respectively (see Fig. 1(a) and (b)).

To this purpose, let us recall that, by reciprocity, the electric field E_θ produced at a point P of spherical coordinates (r, θ, ϕ) by the current $\mathbf{J}_{\rm ring}$ placed on the plane $z = 0$ can be calculated as the reaction of that current with the field $\mathbf{E}'$ that would be produced by an elementary electric test dipole of amplitude $P'_0 = 1$ (A·m) placed at P and directed along the unit vector $\boldsymbol{\theta}_0$:

$$P'_0\, E_\theta(r,\theta,\phi) = \int_{\rm source} \mathbf{E}' \cdot \mathbf{J}_{\rm ring} {\rm d}V = P_0 \int_0^{2\pi} E'_z(\rho = a, \phi, z = 0) e^{-j\ell\phi} {\rm d}\phi \quad (6)$$

If the test dipole is located in the far region, the field incident on the source is, to the dominant asymptotic order, that of a vertically polarized plane wave impinging from the (θ, ϕ) direction having an electric-field amplitude $P'_0 E_0(r) = jk_0\eta_0 P'_0 \exp(-jk_0\, r)/(4\pi r)$. Furthermore, thanks to the azimuthal symmetry of the problem, we may assume that such a plane wave propagates in the xz plane (i.e., $\phi = 0$):

$$\mathbf{E}^{\rm in}(x,z) = P'_0\, E_0(r)\, [\cos\theta \mathbf{x}_0 - \sin\theta \mathbf{z}_0]\, e^{j(k_x x + k_z z)} \quad (7)$$

with $k_x = k_0 \sin\theta$, $k_z = k_0 \cos\theta$, since the far field $E_\theta(r, \theta, \phi)$ at any other azimuthal angle ϕ will be equal to $E_\theta(r, \theta, \phi = 0)$ times $\exp(-j\ell\phi)$.

The field E'_z can then readily be calculated by using a transmission-line (TL) model, wherein the voltage $V(z)$ is associated to the field E'_x and the current $I(z)$ is associated to the field H'_y, as

$$E'_z(x, z = 0) = \frac{k_x}{\omega\varepsilon} H'_y(x, z = 0) = \eta \sin\theta I(0) e^{jk_x x} \quad (8)$$

where η is the characteristic impedance of the medium where the source is located and $I(0)$ indicates the equivalent TL current produced at the source vertical abscissa $z = 0$ by an incident voltage wave of amplitude $P'_0 E_0(r) \cos\theta$.

Inserting (8) into (6) one then has

$$E_\theta(r,\theta,\phi) = P_0 \eta \sin\theta I(0) \int_0^{2\pi} e^{jk_0 a \sin\theta\cos\phi} e^{-j\ell\phi} {\rm d}\phi = 2\pi j^\ell P_0 \eta \sin\theta I(0) J_\ell\,(k_0 a \sin\theta) \quad (9)$$

where a standard integral representation of the Bessel function J_ℓ has been used [57, Eq. 10.9.2].

When the ring source is placed in free space, we have a single, infinite TL with the vertical wavenumber $k_{z0} = k_0 \cos\theta$ and (TM) characteristic admittance $Y_0^{\rm TM} = 1/(\eta_0 \cos\theta)$ (see Fig. 1(a)). It then immediately results

$$I(0) = -\frac{1}{\eta_0} P'_0 E_0(r), \quad (10)$$

from which (3) is obtained.

When the ring source is placed inside an FPCA, the relevant TL model is the one shown in Fig. 1(b). A straightforward network analysis then gives

$$I(0) = \frac{2jY_0 Y_\varepsilon P'_0 E_0(r) \cos\theta e^{jk_0 h\cos\theta}}{(Y_0 + Y_{\rm PRS}) \sin(k_{z\varepsilon} h) - jY_\varepsilon \cos(k_{z\varepsilon} h)} \quad (11)$$

where $k_{z\varepsilon} = k_0\sqrt{\varepsilon_r - \sin^2\theta}$ is the vertical wavenumber inside the cavity, $Y_\varepsilon = k_0\varepsilon_r/(\eta_0 k_{z\varepsilon})$ is the TL admittance inside the cavity, and $Y_{\rm PRS}$ it the TM surface (transition) admittance of the PRS (we are assuming here that the PRS introduces no TM/TE cross-coupling). By comparing (10) with (11), the pattern function in (4) can be obtained with a few algebraic steps.

REFERENCES

[1] L. Allen, M. W. Beijersbergen, R. J. C. Spreeuw, and J. P. Woerdman, "Orbital angular momentum of light and the transformation of Laguerre–Gaussian laser modes," *Phys. Rev. A, Gen. Phys.*, vol. 45, no. 11, pp. 8185–8189, Jun. 1992.

[2] A. M. Yao and M. J. Padgett, "Orbital angular momentum: Origins, behavior and applications," *Adv. Opt. Photon.*, vol. 3, no. 2, pp. 161–204, May 2011.

[3] J. Arlt, V. Garces-Chavez, W. Sibbett, and K. Dholakia, "Optical micromanipulation using a bessel light beam," *Opt. Commun.*, vol. 197, nos. 4–6, pp. 239–245, Oct. 2001.

[4] K. Volke-Sepulveda, V. Garcés-Chávez, S. Chávez-Cerda, J. Arlt, and K. Dholakia, "Orbital angular momentum of a high-order bessel light beam," *J. Opt. B, Quantum Semiclass. Opt.*, vol. 4, no. 2, pp. S82–S89, Apr. 2002.

[5] J. T. Barreiro, T.-C. Wei, and P. G. Kwiat, "Beating the channel capacity limit for linear photonic superdense coding," *Nature Phys.*, vol. 4, no. 4, pp. 282–286, Apr. 2008.

[6] J. Leach, B. Jack, J. Romero, A. K. Jha, A. M. Yao, S. Franke-Arnold, D. G. Ireland, R. W. Boyd, S. M. Barnett, and M. J. Padgett, "Quantum correlations in optical angle-orbital angular momentum variables," *Science*, vol. 329, no. 5992, pp. 662–665, Aug. 2010.

[7] M. Ornigotti, C. Conti, and A. Szameit, "Effect of orbital angular momentum on nondiffracting ultrashort optical pulses," *Phys. Rev. Lett.*, vol. 115, no. 10, Sep. 2015, Art. no. 100401.

[8] R. M. Henderson, "Let's do the twist!: Radiators, experiments, and techniques to generate twisted waves at radio frequencies," *IEEE Microw. Mag.*, vol. 18, no. 4, pp. 88–96, Jun. 2017.

[9] A. Trichili, K.-H. Park, M. Zghal, B. S. Ooi, and M.-S. Alouini, "Communicating using spatial mode multiplexing: Potentials, challenges, and perspectives," *IEEE Commun. Surveys Tuts.*, vol. 21, no. 4, pp. 3175–3203, 4th Quart., 2019.

[10] L. Li and F. Li, "Beating the Rayleigh limit: Orbital-angular-momentum based super-resolution diffraction tomography," *Phys. Rev. E, Stat. Phys. Plasmas Fluids Relat. Interdiscip. Top.*, vol. 88, no. 3, 033205, Sep. 2013.

[11] G. Guo, W. Hu, and X. Du, "Electromagnetic vortex based radar target imaging," (in Chinese), *J. Nat. Univ. Defense Techn.*, vol. 35, no. 6, pp. 71–76, 2013.

[12] K. Liu, Y. Cheng, Z. Yang, H. Wang, Y. Qin, and X. Li, "Orbital-angular-momentum-based electromagnetic vortex imaging," *IEEE Antennas Wireless Propag. Lett.*, vol. 14, pp. 711–714, 2015.

[13] G. A. Turnbull, D. A. Robertson, G. M. Smith, L. Allen, and M. J. Padgett, "The generation of free-space Laguerre–Gaussian modes at millimetre-wave frequencies by use of a spiral phaseplate," *Opt. Commun.*, vol. 127, nos. 4–6, pp. 183–188, Jun. 1996.

[14] F. Tamburini, E. Mari, B. Thidé, C. Barbieri, and F. Romanato, "Experimental verification of photon angular momentum and vorticity with radio techniques," *Appl. Phys. Lett.*, vol. 99, no. 20, Nov. 2011, Art. no. 204102.

[15] R. Niemiec, C. Brousseau, K. Mahdjoubi, O. Emile, and A. Menard, "Characterization of an OAM flat-plate antenna in the millimeter frequency band," *IEEE Antennas Wireless Propag. Lett.*, vol. 13, pp. 1011–1014, 2014.

[16] X. Hui, S. Zheng, Y. Hu, C. Xu, X. Jin, H. Chi, and X. Zhang, "Ultralow reflectivity spiral phase plate for generation of millimeter-wave OAM beam," *IEEE Antennas Wireless Propag. Lett.*, vol. 14, pp. 966–969, 2015.

[17] W.-J. Byun, B. S. Kim, Y.-S. Lee, M. S. Kang, K. S. Kim, and Y. H. Cho, "Simple generation of orbital angular momentum modes with azimuthally deformed Cassegrain subreflector," *Electron. Lett.*, vol. 51, no. 19, pp. 1480–1482, Sep. 2015.
[18] E. Mari, F. Spinello, M. Oldoni, R. A. Ravanelli, F. Romanato, and G. Parisi, "Near-field experimental verification of separation of OAM channels," *IEEE Antennas Wireless Propag. Lett.*, vol. 14, pp. 556–558, 2015.
[19] W. J. Byun, K. S. Kim, B. S. Kim, Y. S. Lee, M. S. Song, H. D. Choi, and Y. H. Cho, "Multiplexed Cassegrain reflector antenna for simultaneous generation of three orbital angular momentum (OAM) modes," *Sci. Rep.*, vol. 6, no. 1, p. 27339, Jun. 2016.
[20] S. Zheng, X. Hui, X. Jin, H. Chi, and X. Zhang, "Transmission characteristics of a twisted radio wave based on circular traveling-wave antenna," *IEEE Trans. Antennas Propag.*, vol. 63, no. 4, pp. 1530–1536, Apr. 2015.
[21] Z. Zhang, S. Zheng, X. Jin, H. Chi, and X. Zhang, "Generation of plane spiral OAM waves using traveling-wave circular slot antenna," *IEEE Antennas Wireless Propag. Lett.*, vol. 16, pp. 8–11, 2017.
[22] L. Gui, M. R. Akram, D. Liu, C. Zhou, Z. Zhang, and Q. Li, "Circular slot antenna systems for OAM waves generation," *IEEE Antennas Wireless Propag. Lett.*, vol. 16, pp. 1443–1446, 2017.
[23] Z. Chang, B. You, L.-S. Wu, M. Tang, Y.-P. Zhang, and J.-F. Mao, "A reconfigurable graphene reflectarray for generation of vortex THz waves," *IEEE Antennas Wireless Propag. Lett.*, vol. 15, pp. 1537–1540, 2016.
[24] S. Yu, L. Li, G. Shi, C. Zhu, X. Zhou, and Y. Shi, "Design, fabrication, and measurement of reflective metasurface for orbital angular momentum vortex wave in radio frequency domain," *Appl. Phys. Lett.*, vol. 108, no. 12, Mar. 2016, Art. no. 121903.
[25] S. Yu, L. Li, G. Shi, C. Zhu, and Y. Shi, "Generating multiple orbital angular momentum vortex beams using a metasurface in radio frequency domain," *Appl. Phys. Lett.*, vol. 108, no. 24, Jun. 2016, Art. no. 241901.
[26] S. Yu, L. Li, and N. Kou, "Generation, reception and separation of mixed-state orbital angular momentum vortex beams using metasurfaces," *Opt. Mater. Expr.*, vol. 7, no. 9, pp. 3312–3321, 2017.
[27] M. L. N. Chen, L. J. Jiang, and W. E. I. Sha, "Quasi-continuous metasurfaces for orbital angular momentum generation," *IEEE Antennas Wireless Propag. Lett.*, vol. 18, no. 3, pp. 477–481, Mar. 2019.
[28] M. L. N. Chen, L. J. Jiang, and W. E. I. Sha, "Generation of orbital angular momentum by a point defect in photonic crystals," *Phys. Rev. A, Gen. Phys. Appl.*, vol. 10, no. 1, Jul. 2018.
[29] F. Shen, J. Mu, K. Guo, S. Wang, and Z. Guo, "Generation of continuously variable-mode vortex electromagnetic waves with three-dimensional helical antenna," *IEEE Antennas Wireless Propag. Lett.*, vol. 18, no. 6, pp. 1091–1095, Jun. 2019.
[30] R. Cicchetti, A. Faraone, and O. Testa, "Near field synthesis based on multi-port antenna radiation matrix eigenfields," *IEEE Access*, vol. 7, pp. 62184—62197, 2019.
[31] B. Thidé, H. Then, J. Sjöholm, K. Palmer, J. Bergman, T. D. Carozzi, Y. N. Istomin, N. H. Ibragimov, and R. Khamitova, "Utilization of photon orbital angular momentum in the low-frequency radio domain," *Phys. Rev. Lett.*, vol. 99, no. 8, p. 08071, Aug. 2007.
[32] S. M. Mohammadi, L. K. S. Daldorff, J. E. S. Bergman, R. L. Karlsson, B. Thidé, K. Forozesh, T. D. Carozzi, and B. Isham, "Orbital angular momentum in radio—A system study," *IEEE Trans. Antennas Propag.*, vol. 58, no. 2, pp. 565–572, Feb. 2010.
[33] A. Tennant and B. Allen, "Generation of OAM radio waves using circular time-switched array antenna," *Electron. Lett.*, vol. 48, no. 21, pp. 1365–1366, Oct. 2012.
[34] Q. Bai, A. Tennant, and B. Allen, "Experimental circular phased array for generating OAM radio beams," *Electron. Lett.*, vol. 50, no. 20, pp. 1414–1415, Sep. 2014.
[35] M. Barbuto, F. Trotta, F. Bilotti, and A. Toscano, "Circular polarized patch antenna generating orbital angular momentum," *Prog. Electromagn. Res.*, vol. 148, pp. 23–30, Jun. 2014.
[36] C. L. Qin, M. Huang, J. J. Yang, L. Shen, and Y. H. Liang, "Generation of OAM radio waves using patch antenna," *Adv. Mater. Res.*, vols. 926–930, pp. 2337–2340, May 2014.
[37] K. Liu, H. Liu, Y. Qin, Y. Cheng, S. Wang, X. Li, and H. Wang, "Generation of OAM beams using phased array in the microwave band," *IEEE Trans. Antennas Propag.*, vol. 64, no. 9, pp. 3850–3857, Sep. 2016.
[38] Z. Zhao, G. Xie, L. Li, H. Song, C. Liu, K. Pang, R. Zhang, C. Bao, Z. Wang, S. Sajuyigbe, S. Talwar, H. Nikopour, and A. E. Willner, "Performance of using antenna arrays to generate and receive mm-Wave orbital-angular-momentum beams," in *Proc. IEEE Global Commun. Conf. (GLOBECOM)*, Singapore, Dec. 2017, pp. 1–6.
[39] W. Cheng, H. Zhang, L. Liang, H. Jing, and Z. Li, "Orbital-angular-momentum embedded massive MIMO: Achieving multiplicative spectrum-efficiency for mmWave communications," *IEEE Access*, vol. 6, pp. 2732–2745, 2018.
[40] D. Liu, L. Gui, Z. Zhang, H. Chen, G. Song, and T. Jiang, "Multiplexed OAM wave communication with two-OAM-mode antenna systems," *IEEE Access*, vol. 7, pp. 4160–4166, 2019.
[41] T. Yuan, H. Wang, Y. Qin, and Y. Cheng, "Electromagnetic vortex imaging using uniform concentric circular arrays," *IEEE Antennas Wireless Propag. Lett.*, vol. 15, pp. 1024–1027, 2016.
[42] Y. Qin, K. Liu, Y. Cheng, X. Li, H. Wang, and Y. Gao, "Sidelobe suppression and beam collimation in the generation of vortex electromagnetic waves for radar imaging," *IEEE Antennas Wireless Propag. Lett.*, vol. 16, pp. 1289–1292, 2017.
[43] S. Guo, Z. He, and R. Chen, "High resolution 2-D electromagnetic vortex imaging using uniform circular arrays," *IEEE Access*, vol. 7, pp. 132430–132437, 2019.
[44] S. Guo, Z. He, Z. Fan, and R. Chen, "CUCA based equivalent fractional order OAM mode for electromagnetic vortex imaging," *IEEE Access*, vol. 8, pp. 91070–91075, May 2020.
[45] D. R. Jackson and A. A. Oliner, "Leaky-wave antennas," in *Modern Antenna Handbook*, C. A. Balanis, Ed. Hoboken, NJ, USA: Wiley, 2008, ch. 7, pp. 325–367.
[46] A. Galli, P. Baccarelli, and P. Burghignoli, "Leaky-wave antennas," in *The Wiley Encyclopedia of Electrical and Electronics Engineering*, J. Webster, Ed. New York, NY, USA: Wiley, 2016.
[47] A. Ip and D. R. Jackson, "Radiation from cylindrical leaky waves," *IEEE Trans. Antennas Propag.*, vol. 38, no. 4, pp. 482–488, Apr. 1990.
[48] P. Burghignoli, W. Fuscaldo, D. Comite, P. Baccarelli, and A. Galli, "Higher-order cylindrical leaky waves—Part I: Canonical sources and radiation formulas," *IEEE Trans. Antennas Propag.*, vol. 67, no. 11, pp. 6735–6747, Nov. 2019.
[49] P. Burghignoli, D. Comite, W. Fuscaldo, P. Baccarelli, and A. Galli, "Higher-order cylindrical leaky waves—Part II: Circular array design and validations," *IEEE Trans. Antennas Propag.*, vol. 67, no. 11, pp. 6748–6760, Nov. 2019.
[50] W. Fuscaldo, S. Tofani, D. C. Zografopoulos, P. Baccarelli, P. Burghignoli, R. Beccherelli, and A. Galli, "Systematic design of THz leaky-wave antennas based on homogenized metasurfaces," *IEEE Trans. Antennas Propag.*, vol. 66, no. 3, pp. 1169–1178, Mar. 2018.
[51] O. Luukkonen, C. Simovski, G. Granet, G. Goussetis, D. Lioubtchenko, A. V. Raisanen, and S. A. Tretyakov, "Simple and accurate analytical model of planar grids and high-impedance surfaces comprising metal strips or patches," *IEEE Trans. Antennas Propag.*, vol. 56, no. 6, pp. 1624–1632, Jun. 2008.
[52] J. Kane, "A surface wave antenna as a boundary value problem," in *Proc. Symp. EM Theory Antennas*, E. C. Jordan, Ed. London, U.K.: Pergamon Press, 1963, pt. 2, pp. 891–894.
[53] D. Comite, P. Burghignoli, P. Baccarelli, and A. Galli, "2-D beam scanning with cylindrical-leaky-wave-enhanced phased arrays," *IEEE Trans. Antennas Propag.*, vol. 67, no. 6, pp. 3797–3808, Jun. 2019.
[54] D. Comite, S. K. Podilchak, M. Kuznetcov, V. Gómez-Guillamón Buendía, P. Burghignoli, P. Baccarelli, and A. Galli, "Wideband array-fed Fabry–Pérot cavity antenna for 2-D beam steering," *IEEE Trans. Antennas Propag.*, early access, Jul. 17, 2020, doi: 10.1109/TAP.2020.3008764.
[55] R. Sorrentino, "Transverse resonance technique," in *Numerical Techniques for Microwave and Millimeter-Wave Passive Structures*, T. Itoh, Ed. New York, NY: Wiley, 1989, ch. 11.
[56] D. Comite, P. Burghignoli, P. Baccarelli, D. Di Ruscio, and A. Galli, "Equivalent-network analysis of propagation and radiation features in wire-medium loaded planar structures," *IEEE Trans. Antennas Propag.*, vol. 63, no. 12, pp. 5573–5585, Dec. 2015.
[57] Sec. 10 (Bessel Functions). *NIST Digital Library of Mathematical Functions*. Accessed: Apr. 10, 2020. [Online]. Available: http://dlmf.nist.gov/10

PAOLO BURGHIGNOLI (Senior Member, IEEE) was born in Rome, Italy, in 1973. He received the Laurea degree *(cum laude)* in electronic engineering and the Ph.D. degree in applied electromagnetics from the Sapienza University of Rome, Rome, in 1997 and 2001, respectively.

In 1997, he joined the Department of Information Engineering, Electronics and Telecommunications, Sapienza University of Rome. In 2004, he was a Visiting Research Assistant Professor with the University of Houston, Houston, TX, USA. From 2010 to 2015, he was an Assistant Professor with the Sapienza University of Rome, where he has been an Associate Professor, since October 2015. In March 2017, he received the National Scientific Qualification for the role of a Full Professor of electromagnetic fields in Italian Universities. He has authored about 250 papers in international journals, books, and conference proceedings. His current research interests include analysis and design of planar antennas and arrays, leakage phenomena in uniform and periodic structures, numerical methods for integral equations and periodic structures, propagation and radiation in metamaterials, electromagnetic shielding, transient electromagnetic waves, and graphene electromagnetics.

Dr. Burghignoli was a recipient of the Giorgio Barzilai Laurea Prize presented by the former IEEE Central & South Italy Section, from 1996 to 1997, the 2003 IEEE MTT-S Graduate Fellowship, and the 2005 Raj Mittra Travel Grant for Junior Researchers presented at the IEEE AP-S Symposium on Antennas and Propagation, Washington, DC, USA. He was the Secretary of the European Microwave Week in 2009 (EuMW 2009) and a member of the Organizing Committee and the Scientific Board of the PhotonIcs & Electromagnetics Research Symposium in 2019 (PIERS 2019). In 2016, he was recognized as an Outstanding Reviewer for the IEEE TRANSACTIONS ON ANTENNAS AND PROPAGATION by the IEEE Antennas and Propagation Society. He is currently an Associate Editor of *IET Electronics Letters* (Institution of Engineering and Technology) and the *International Journal of Antennas and Propagation* (Hindawi).

WALTER FUSCALDO (Member, IEEE) received the M.Sc. *(cum laude)* degree in telecommunications engineering from the Sapienza University of Rome, Rome, in 2013, and the Ph.D. degree (*cum laude* and with the *Doctor Europaeus* label) in information and communication technology (applied electromagnetics curriculum) from the Department of Information Engineering, Electronics and Telecommunications (DIET) and the Institut d'Électronique et de Télécommunications de Rennes (IETR), Université de Rennes 1, Rennes, France, under a cotutelle agreement between the institutions.

In 2014, 2017, and 2018, he was a Visiting Researcher with the NATO-STO Center for Maritime Research and Experimentation, La Spezia, Italy. In 2016, he was a Visiting Researcher with the University of Houston, Houston, TX, USA. Since July 2017, he has been a Postdoctoral Researcher with the Sapienza University of Rome, and in July 2020, he joined the Institute for Microelectronics and Microsystems (IMM), Rome, Italy, as a Researcher of the National Research Council of Italy. His current research interests include propagation of leaky waves, surface waves and surface plasmon polaritons, analysis and design of leaky-wave antennas, generation of localized electromagnetic waves, graphene electromagnetics, metasurfaces, and THz antennas.

Dr. Fuscaldo was awarded several prizes, among which the prestigious Young Engineer Prize for the Best Paper presented at the 46th European Microwave Conference in 2016, London, U.K. He is currently an Associate Editor of the journals *IET Microwaves, Antennas and Propagation*, and *Electronics Letters*.

FRANCESCO MANCINI received the M.Sc. degree *(cum laude)* in electronic engineering from the Sapienza University of Rome, Rome, in 2020.

In December 2019, he joined Leonardo S.p.A., as a System Engineer. His research interests include Fabry-Perot cavity antennas, leaky-wave antennas, frequency selective surfaces, and higher-order cylindrical leaky-waves.

DAVIDE COMITE (Senior Member, IEEE) received the master's degree *(cum laude)* in telecommunications engineering and the Ph.D. degree in electromagnetics and mathematical models for engineering from the Sapienza University of Rome, Rome, Italy, in 2011 and 2015, respectively.

He is currently a Postdoctoral Researcher with the Sapienza University of Rome. He was a Visiting Ph.D. Student with the Institute of Electronics and Telecommunications of Rennes, University of Rennes 1, France, from March to June 2014, and a Postdoctoral Researcher with the Center of Advanced Communications, Villanova University, PA, USA, in 2015. His scientific interests include the study and design of leaky-wave antennas, 2-D periodic leaky-wave antennas, and the generation of non-diffracting waves and pulses. He is also interested in the study of the scattering from natural surfaces, the GNSS reflectometry, and radar altimeter applications over the land. His activity also regards microwave imaging and objects detection performed through GPR, and the modeling of the radar signature in forward scatter radar systems.

Dr. Comite is a Senior Member of URSI. He was a recipient of a number of awards at national and international conferences. Most recently, he received the Young Scientist Award at URSI GASS 2020. He received the Publons Top Peer Reviewers Award for both Geoscience and Engineering, in September 2018, and for Cross-fields in 2019. In 2019 and 2020, he was recognized as an Outstanding Reviewer for the IEEE TRANSACTIONS ON ANTENNAS AND PROPAGATION by the IEEE Antennas and Propagation Society. In 2020, he was awarded as the Best Reviewer for the IEEE JOURNAL OF SELECTED TOPICS IN APPLIED EARTH OBSERVATIONS AND REMOTE SENSING. He currently serves as a reviewer for several international journals. He is also an Associate Editor of the *IET Journal of Engineering*, the *IET Microwaves, Antennas and Propagation* by the Institution of Engineering and Technology, and IEEE ACCESS.

PAOLO BACCARELLI (Member, IEEE) received the Laurea degree in electronic engineering and the Ph.D. degree in applied electromagnetics from the La Sapienza University of Rome, Rome, Italy, in 1996 and 2000, respectively.

In 1996, he joined the Department of Electronic Engineering, La Sapienza University of Rome, where he has been an Assistant Professor, since November 2010. From April 1999 to October 1999, he was a Visiting Researcher with the University of Houston, Houston, TX, USA. In 2017, he joined the Department of Engineering, University of Rome Tre, Rome, where he has been an Associate Professor, since July 2017. In December 2017, he received the

National Scientific Qualification for the role of Full Professor of Electromagnetic Fields in Italian Universities. He has coauthored over 250 articles in international journals, conference proceedings, and book chapters. His research interests include analysis and design of planar antennas and arrays, leakage phenomena in uniform and periodic structures, numerical methods for integral equations and periodic structures, propagation and radiation in anisotropic media, metamaterials, graphene, and electromagnetic band-gap structures.

Dr. Baccarelli has been a member of the TPCs of several international conferences. He was a recipient of the Giorgio Barzilai Laurea Prize, from 1994 to 1995, presented by the former IEEE Central and South Italy Section. He is an Associate Editor of the *Electronics* (MDPI) and the *International Journal of Antennas and Propagation* (Hindawi). He was a Secretary of the 2009-European Microwave Week (EuMW 2009).

ALESSANDRO GALLI (Member, IEEE) received the Laurea degree in electronic engineering and the Ph.D. degree in applied electromagnetics from the Sapienza University of Rome, Rome, Italy, in 1990 and 1994, respectively.

Since 1990, he has been with the Department of Information Engineering, Electronics and Telecommunications, Sapienza University of Rome. In 2000, he became an Assistant Professor and an Associate Professor, in 2002, in the sector of Electromagnetic Fields with the Sapienza University of Rome, where he passed the National Scientific Qualification, in 2012, and then in 2020, he definitively achieved the role of Full Professor. He is currently teaching or coteaching the courses of electromagnetic fields, advanced antenna engineering, microwaves, and engineering electromagnetics, for Bachelor and Master degrees in electronics engineering and in communications engineering at Sapienza University. He has authored about 300 papers in international journals, books, and conference proceedings. He holds a patent for an invention of a type of microwave leaky-wave antenna. His current research interests include theoretical and applied electromagnetics regarding guided waves, propagation and radiation problems, mainly focused on modeling, numerical analysis, and design of antennas and passive devices from microwaves to terahertz. His specific topics involve leaky waves and leaky-wave antennas, periodic and multilayered printed structures, beam focusing devices including complex media, metamaterials and graphene. His research activities also concern the areas of geoelectromagnetics, bioelectromagnetics, and plasma heating.

Dr. Galli was elected as the Italian Representative of the Board of Directors of the European Microwave Association (EuMA), the main European Society of electromagnetics, for the 2010–2012 triennium, and then re-elected for the 2013–2015 triennium. He is also a member of the board of the European School of Antennas (ESoA) and of the leading scientific societies of electromagnetics. He was the General Co-Chair of the European Microwave Week, the most important conference event in the electromagnetic area at European level, in 2014. Since its foundation in 2012, he has been the Coordinator of the European Courses on Microwaves, the first European educational institution on microwaves. He is currently an Associate Editor of the *International Journal of Microwave and Wireless Technologies* (Cambridge University Press) and of *IET Microwaves, Antennas and Propagation* (Institution of Engineering and Technology). He was a recipient of various grants and prizes for his research activity, such as the Barzilai Prize for the best scientific work of under-35 researchers at the 10th National Meeting of Electromagnetics, in 1994, and the Quality Presentation Recognition Award at the International Microwave Symposium by the Microwave Theory and Techniques Society of the IEEE, in 1994 and 1995. Based on a poll among about 300 attendants to the ESoA courses in a competition of more than 100 international speakers, he has been elected as the ESoA Best Teacher, in 2017.